HHS Public Access

Author manuscript

FASEB J. Author manuscript; available in PMC 2021 September 01.

Published in final edited form as:

FASEB J. 2020 September ; 34(9): 11900–11912. doi:10.1096/fj.201903220R.

Novel evidence for Retinoic Acid-Induced G (Rig-G) as a tumor suppressor by activating p53 signaling pathway in lung cancer

Junjun Sun[1,*], **Xuan Wang**[2,*], **Wenfang Liu**[3,*], **Ping Ji**[1], **Anquan Shang**[1], **Junlu Wu**[1], **Hao Zhou**[3], **Wenqiang Quan**[1], **Yiwen Yao**[1], **Yibao Yang**[1], **ChenZheng Gu**[1], **Zujun Sun**[1], **Ajay Goel**[4], **Wenhao Weng**[5,6], **Dong Li**[1]

[1]Department of Clinical Laboratory, Shanghai Tongji Hospital, Tongji University School of Medicine, Shanghai 200065, China.

[2]Department of Pharmacy, Putuo People's Hospital, Shanghai 200060, China.

[3]Department of General Surgery, Shanghai Tongji Hospital, Tongji University School of Medicine, Shanghai 200065, China.

[4]Department of Molecular Diagnostics and Experimental Therapeutics, Beckman Research Institute of City of Hope Comprehensive Cancer Center, Duarte, CA, USA

[5]Department of Clinical Laboratory, Yangpu Hospital, Tongji University School of Medicine, Shanghai, 200090, China.

[6]Institute of Gastrointestinal Surgery and Translational Medicine, Yangpu Hospital, Tongji University School of Medicine, Shanghai, 200090, China.

Abstract

Lung cancer is one of most common malignancies worldwide. We have previously identified retinoic acid-induced gene G (Rig-G) as a tumor suppressor in not only acute promyelocytic leukemia, but as well in other solid tumors. However, the clinical significance of Rig-G and the underlying mechanism(s) for its biological function in lung cancer remain largely unexplored. Herein, we first compared the expression of Rig-G between lung cancer (n=138) and normal tissues (n=23), from public-available datasets and our patient cohort. We further analyzed the correlation of Rig-G expression with key clinico-pathological features and survival outcomes in a multi-site clinical cohort of 300 lung cancer patients. Functional studies for Rig-G were performed in cell lines, and an animal model to support clinical findings. We found that Rig-G was frequently downregulated in lung cancer tissues and cell lines, and correlated with poor prognosis in lung cancer patients. Overexpression of Rig-G led to significantly reduced cell growth and suppressed

Corresponding authors: **Ajay Goel**, PhD, Department of Molecular Diagnostics and Experimental Therapeutics, Beckman Research Institute of City of Hope Comprehensive Center; 1218 S. Fifth Avenue, Suite 2226, Biomedical Research Center, Monrovia, CA 91016; Phone: 626-218-3452; ajgoel@coh.org. **Wenhao Weng**, PhD, Department of Clinical Laboratory, Yangpu Hospital, Tongji University School of Medicine, 450 tenyue Road, Shanghai, 200090, China. Phone: 86-21-65690520, Fax: 86-21-65690520, wengwenhao2010@hotmail.com; or **Dong Li**, PhD, Department of Clinical Laboratory, Shanghai Tongji Hospital, Tongji University School of Medicine, 389 Xincun Road, Shanghai 200065, China. Tel 86-21-66111425, Fax 86-21-56051814, lidong@tongji.edu.cn.

*These authors contributed equally to this work.

Author contributions: Study concept and design, analysis and interpretation of data and statistical analysis: JJS, WHW, AG and DL; Specimen provider and acquisition of clinical data: WFL; *In vivo* and *in vitro* experiments: XW, PJ, AQS, JLW, HZ, WQQ, YWY, YBY, CZG, ZJS, WHW; Drafting of the manuscript: WHW and AG.

Conflicts of Interest: None of the authors have any potential conflicts to disclose.

migration in A549 and NCI-H1944 cells, accompanied by reduced epithelial-mesenchymal transition. Likewise, restoration of Rig-G in Lewis lung carcinoma cells permitted development of fewer cancer metastases *vs.* controls in an animal model. Gene expression profiling results identified p53 pathway as a key downstream target of Rig-G, and p53 inhibition by pifithrin-α caused abrogation of tumor-suppressive effects of Rig-G in lung cancer. In conclusion, we for the first time have identified Rig-G as a novel and important tumor suppressor, which may serve as a potential therapeutic target for restoring p53 expression in lung cancer patients.

Keywords

Rig-G; lung adenocarcinoma; p53; epithelial-mesenchymal transition; metastasis; prognosis; therapy

1. Introduction

Lung cancer is currently one of most common causes of cancer-related morbidity and mortality worldwide[1]. In China, incidence and mortality rates from lung cancer have been increasing rapidly for decades, possibly due to lifestyle-related risk factors such as tobacco smoking, or air pollution[2]. Despite recent advances in the early disease detection and availability of targeted therapies such as EGFR tyrosine kinase inhibitors, patients with lung cancer are often diagnosed at advanced stages and their overall prognosis remains quite poor. Currently, the 5-year survival rates in lung cancer patients are about 15%, highlighting the imperative need to identify additional therapeutic strategies for an improved cure and management of this malignancy[3, 4]. It is worth noting that advanced lung cancers tend to spread to brain, liver or bones; and approximately 15% patients with metastatic disease only survive for an average of 1 year post-surgery, with almost no long term survivors[5]. Therefore, identification of previously unrecognized molecular targets that drive lung cancer development, particularly metastasis, would not just be of biological relevance, but will offer tremendous clinical significance as these will propel new drug development for a more effective treatment of this deadly disease.

The retinoic acid-induced gene G (RIG-G) was originally identified from an acute promyelocytic leukemia cell line NB4, treated with an all-trans retinoic acid (ATRA)[6]. Intriguingly, in addition to ATRA, interferon α (IFNα) can dramatically induce Rig-G expression in hematopoietic cell lines, as well as in other types of cancer cells[6, 7]. Furthermore, we have previously shown that Rig-G has anti-tumor activity in various types of cancer cells through cell cycle inhibition and via up-regulation of p21 and p27 expression[8–10], implying that Rig-G may serve as a tumor suppressor in lung cancer. However, the clinical significance of Rig-G and the underlying mechanism(s) for its biological function in lung cancer remains largely unexplored.

Herein, we envisaged to interrogate the molecular contributions of Rig-G in lung adenocarcinoma, clarify its molecular function, uncover novel downstream target(s) of Rig-G, and decipher whether these genes may have any translational relevance as disease biomarkers or therapeutic targets in lung adenocarcinoma.

2. Material and Methods

2.1 Lung cancer tissues, cell culture and chemicals

For the comparison of Rig-G expression between cancer and normal tissues, the cancer tissues and matched adjacent normal tissues were obtained from lung cancer patients enrolled at the Department of General Surgery, Shanghai Tongji Hospital. A written informed consent was obtained from all patients and the study was approved by ethics committee of Shanghai Tongji Hospital. The human NSCLC cell lines (A549, H1792, SK-MES-1 and NCI-H1944), human embryonic lung fibroblast cells (MRC-5), and mouse cells (LLC) were obtained from the American Type Tissue Collection (ATCC, Manassas, VA, USA). The cells were cultured in Dulbecco's modified Eagle's medium (DMEM, Hyclone Laboratories, Inc., South UT, USA) supplemented with 10% fetal bovine serum (FBS, Invitrogen, Grand Island, NY, USA), 100 U/mL penicillin and 100 U/mL streptomycin (Hyclone Laboratories, Inc., South UT, USA). Cell cultures were performed at 37°C in humidified air with 5% CO_2. Cyclic pifithrin-α-p-nitro were purchased from Abcam (Cambridge, UK).

2.2 Construction of lentiviral vector and Transfection

The pLenti6/TO/V5-DEST, Packaging Mix, LR clonase II, Lipofectamine 2000 are obtained from Invitrogen (Grand Island, NY, USA). Rig-G was successfully cloned into lentiviral vectors using LR recombination system. The virus was produced by co-transfecting pLenti6/TO/V5-GIM-RIG-G with the packaging mix into 293T cells, using Lipofectamine 2000. The viral particles were harvested and used to infect A549 and NCI-H1944 cells.

2.3 Cell scratch assay

The treated or control cells were plated into 12-well plates and grown to confluency. A wound area was generated by scraping cells with a 10 μl pipette tip across the entire diameter of the dish and extensively rinsed with the medium to remove all cellular debris. Low-serum DMEM with pifithrin-α (10μM) was then added to promote cell proliferation during the experiment and the closing of the wound was observed at different time points. Cells were photographed by a Nikon Eclipse Ti-S fluorescence microscope (Tokyo, Japan) at X100 total magnification, and distance of migrated was measured by using Image Pro Plus (Media Cybernetics, Maryland, USA).

2.4 Transwell migration assay

Cell migration ability was analyzed in a transwell chamber assay. 10% FBS was used as the chemoattractant. The cells on the lower surface of the membrane were fixed with 100% methanol and subsequently stained with hematoxylin and eosin (Njjcbio, China). Cells were photographed by a Nikon Eclipse Ti-S fluorescence microscope (Tokyo, Japan) at X100 total magnification, and counted using Image Pro Plus (Media Cybernetics, Maryland, USA).

2.5 CCK-8 Cell Counting Kit Assay

Treated or control cells were plated in 96-well plates (100 μl/well). A 10 μl cell counting kit assay (Keygentec, China) was added every other day and incubated for 2 h at 37°C in a humidified incubator. Optical density value was measured at 450 nm. Pifithrin-α was then added to promote cell proliferation during the experiment.

2.6 Immunofluorescence staining

For F-actin staining, the adherent cells grown on coverslips were washed in PBS and fixed with 4% formaldehyde for 15 min, followed by washing in PBS. After drying, the cells were permeabilized with PBS containing 0.1%Triton X-100. The CytoPainterPhalloidin-iFluor 555 were diluted in PBS, and incubated with the permeabilized cells for 1 h. All incubations were carried out at room temperature and followed by three washes in PBS. Finally, the slides were mounted with 5 μl mounting medium containing DAPI (Vector Laboratories, Burlingame, CA, USA) and examined by microscopy (Olympus BX51, Tokyo, Japan) with CCD camera (Model 4.2, Diagnostic, USA).

2.7 Immunohistochemical analysis

The following primary antibodies were used for immunohistochemical analysis: rabbit anti-RIG-G (a gift from Dr. Jianhua Tong), rabbit anti-p53 (Santa Cruz Biotechnology, Santa Cruz, CA, USA), mouse anti-Ki-67, mouse anti E-cadherin, and rabbit anti-vimentin (All three antibodies from Cell signaling technology, Boston, USA). The lungs were infused with 4% paraformaldehyde (Carl Roth, Karlsruhe, Germany) and incubated for 24 h. Tissues were embedded in paraffin, sectioned and stained with hematoxylin and eosin. For immunohistochemical analysis, sections were deparaffinized and boiled for 15 min in 0.01 M citrate buffer (pH 6.0) for antigen retrieval. Unspecific tissue peroxidases were blocked by 3% (v/v) H_2O_2. Sections were incubated with primary antibodies in 4℃ overnight. Secondary antibody incubation and staining were performed using the EnVision®+ System–HRP (DAB) kit (Dako, Carpinteria, CA, USA), according to the manufacturer's recommendations. The sections were counterstained with hematoxylin and mounted.

2.8 Tissue microarray analysis

Tissue microarray (ZL-LUC961) was purchased from Shanghai Zhuolibiotech company. Tissue microarray (HLugA180Su06) with complete clinic pathological data was purchased from Shanghai outdo biotech. Evaluation of nuclear p53 expression and Rig-G expression in cytoplasm was performed in accordance with the immunoreactive score (IRS) proposed by Remmele and Stegnerl which modified according to the actual situation: IRS = SI (staining intensity) × PP (percentage of positive cells). SI was determined as 0 is negative; 1, weak; 2, moderate; and 3, strong. PP was defined as 0 is negative; 1, 25% positive cells; 2, 26–50% positive cells; 3, more than 50% positive cells. Ten visual fields from different areas of each tumor were used for the IRS evaluation. Tumor slices scoring 0 to 3 was considered as low expression, 4 to 9 was considered as high expression.

2.9 Western blot analysis

Cells were lysed in cell lysis buffer (cell signaling technology, Boston, USA) supplemented with protease and phosphatase inhibitors (Roche, Germany). Briefly, 30 μg total protein were loaded on 10% SDS polyacrylamide gels, electrophoresed, and blotted onto Hybond-C Extra membranes (Amersham Bioscience, Buckinghamshire, UK). Primary antibodies used for western blot analysis included the following: rabbit anti Rig-G (a gift from Dr. Jianhua Tong), mouse anti-cyclin D1, rabbit anti-p21, mouse anti-E-cadherin, rabbit anti-vimentin, rabbit anti-p-Akt (Ser473), rabbit anti-p-MDM2(Ser166), rabbit anti-Bcl-2, mouse anti-β-actin (all from Cell Signaling Technology) and rabbit anti-p53(Santa Cruz Biotechnology). HRP-conjugated goat anti-rabbit (Santa Cruz Biotechnology) or rabbit anti-mouse (Dako) was used as secondary antibody. Where indicated, cells were treated with pifithrin-α (10μM) prior to protein lysis.

2.10 RNA isolation and real-time PCR analysis

Total RNA was isolated using TRIzol reagent (Life Technologies) following the manufacturer's protocol. Briefly, cDNA was synthesized by reverse transcription using PrimeScript II 1st strand cDNA Synthesis Kit (Takara). Real-time PCR was performed using SYBR® Premix Ex Taq™ II (Takara) on the AB 7300 Real time PCR system machine (AB Applied Biosystems, Singapore). The following PCR primers were used: GAPDH, 5'- CGG AGT CAA CGG ATT TGG TCG TAT-3' and 5'- AGC CTT CTC CAT GGT GGT GAA GAC-3'; Rig-G, 5'-GAA GAA ATG AAA GGG CGA AGG-3' and 5'-AGG ACA TCT GTT TGG CAA GGA G-3'; Glyceraldehyde-3-phosphate dehydrogenase (GAPDH) was used as an internal control. The relative expression levels of mRNA were quantified using the ΔΔCt method.

2.11 mRNA expression array

Total RNA was isolated from A549 and RIG-G expressingA549 cells using TRIzol reagent (Life Technologies) according to the manufacturer's recommendation. Total mRNA was labeled with Cy5 and then hybridized to Human Whole Genome OneArrayTM Version 6.1 (Phalanx Biotech Group, Xinzhu, Taiwan), scanned with an Agilent Microarray scanner (G2505C). Differentially expressed genes with fold changes of >1.0 were applied to pathway enrichment analysis with FunRich. Gene Set Enrichment Analysis was supported by the Broad Institute website (http://www.broadinstitute.org/gsea/index.jsp) and includes versions compatible with Java. All GSEA analyses presented here were performed using the Java GSEA implementation.

2.12 LLC metastatic murine models

Female C57BL/6 mice were obtained from the National Rodent Laboratory Animal Resource (Shanghai Branch, PRC) and maintained at the specific pathogen free (SPF) Central Animal Facility of the Tongji Hospital of Tongji University. This study was conducted in strict accordance with the recommendations depicted in the Guidelines for the Care and Use of Laboratory Animals of the National Institutes of Health in Bethesda, MD, USA. All animal experiments were approved by the Tongji Hospital of Tongji University Ethics Committee on the Use and Care of Animals. All surgeries were performed under

sodium pentobarbital anesthesia, and all efforts were made to minimize suffering. The LLC-Rig-G cells or LLC cells (density: 5×10^5) were injected into the lateral tail veins of 4–5-week-old female C57BL/6 mice. Two weeks later, the mice were euthanized, and tumors were resected and fixed in 3.7% buffered formalin. For tissue morphology evaluation, hematoxylin and eosin staining were performed on sections from embedded samples.

2.13 Statistical analysis

The statistical analyses were carried out by using the GraphPad Prism Ver. 6.0 or Medcalc version 12.3 programs. The statistically significant differences between treated cells and untreated control cells were calculated by unpaired Student t-test or non-parametric Mann–Whitney U test. The chi square ($\chi 2$) test was used to analyze expression correlation of p53 and Rig-G in lung tissue microarray. Kaplan–Meier analysis and log-rank test was used to estimate and compare survival, defined by the time from surgery until death (patients alive were censored at the time of their last follow-up), of patients with Rig-G high expressing and Rig-G low expressing primary tumors. The Cox proportional hazards models were used to estimate HRs for death. $P<0.05$ is determined as statistic significant. All experiments were conducted at least triple times.

3. Results

3.1 The expression level of Rig-G is downregulated in lung cancer tissues and correlates with poor clinical outcomes

To investigate the role of Rig-G in lung cancer, we initially examined its expression levels in cell lines and cancer tissues. As shown in Figure 1A, Rig-G showed significantly lower mRNA or protein levels in lung cancer cell lines A549, H1792, SK-MES-1 and NCI-H1944, than those in normal lung fibroblast cell line MRC-5 ($P<0.01$). We further measured Rig-G expression in matched cancerous and paired healthy tissues by qPCR and IHC assays. The expression of Rig-G was significantly lower in cancer tissues vs. matched healthy tissues ($P<0.01$, Figure 1B). In support of these results, IHC assay also revealed a strong staining for Rig-G in healthy cells, while very weak staining in cancer cells (Figure 1C). To validate these findings, we examined Rig-G expression in a publicly-available dataset GSE83277[11], comprising of 17 normal lung tissues and 132 cancer tissues. Reassuringly, Rig-G expression was significantly downregulated with average a 4.3 fold decrease in cancer vs. normal tissues ($P<0.01$, Figure 1D), suggesting that down-regulation of Rig-G expression may play a critical role in the lung carcinogenesis.

To better understand the clinical significance of Rig-G expression in lung cancer, we analyzed its correlation with various clinicopathological features or patient survival with complete follow-up information. We have examined the expression level of Rig-G in lung cancer tissue microarray (n=85) by immunohistochemistry. We have found that higher expression of Rig-G is correlated with advanced clinical stage (Table 1). Furthermore, patients with lower expression of Rig-G have poor prognosis compared to those with a higher level of Rig-G ($P= 0.0084$, HR= 0.4893, Figure 1E). Collectively, we for the first time have showed that Rig-G expression is frequently down-regulated in lung cancer, and its lower expression is associated with the poor prognosis in lung cancer patients.

3.2 The overexpression of Rig-G inhibits growth and migration in lung cancer cells, and in an animal model

Since Rig-G is often lost in lung cancer, we hypothesized that Rig-G may have a tumor suppressive function in lung carcinogenesis. To confirm this hypothesis, we first successfully established stable Rig-G expressing lung cancer cell lines, A549 and NCI-H1944, by using lentiviral overexpression system. We subsequently performed CCK-8 assay to determine the growth effect of Rig-G overexpression on lung cancer cells. As shown in Figure 2A, the restoration of Rig-G in lung cancer cells significantly slowed down their ability to grow when compared to corresponding controls ($P<0.01$), highlighting that Rig-G protein plays a critical role in suppressing cell proliferation in lung cancer.

To further investigate the biological effects of Rig-G in tumor metastasis, we performed a wound healing assay. Rig-G expressing cells showed a lower migratory potential in this assay vs. controls ($P<0.01$, Figure 2B). Moreover, transwell migration assay demonstrated that overexpression of Rig-G significantly decreased numbers of cells that migrated into the lower chamber ($P<0.01$, Figure 2C). To validate our *in vitro* results, we next used a Lewis lung carcinoma (LLC) murine model, a well-established preclinical model for metastasis study[12], to determine the biological impact of Rig-G in cancer cell metastasis. In support of our previous findings, Rig-G expressing LLC cells developed fewer lung tumor metastases compared to controls, indicating that restoration of Rig-G effectively impaired the ability of LLC cells to metastasize in the animal model ($P<0.01$, Figure 2D). Taken together, our data provide a novel evidence that Rig-G functions as a promising tumor suppressor, which restricts lung cancer progression and metastasis.

3.3 The restoration of Rig-G expression suppresses epithelial–mesenchymal transition (EMT) in lung cancer cells

Accumulating evidence points that cancer metastasis is profoundly related to an evolutionarily conserved developmental program, called epithelial mesenchymal transition (EMT)[13]. Based on the inhibitory effect of Rig-G on metastasis, we therefore examined the expression levels of a key epithelial marker E-cadherin, as well as mesenchymal marker vimentin, in lung cancer cells with or without Rig-G overexpression. We noted that both A549 and NCI-H1944 control cells showed a lower expression of E-cadherin, while higher level of vimentin, indicating these cells possess mesenchymal characteristics. In contrast to controls cells, overexpression of Rig-G in lung cancer cell lines significantly induced E-cadherin expression, while simultaneously suppressing vimentin (Figure 3A). Similarly, the metastatic lung cancer tissues from the mice model revealed an increased E-cadherin expression along with decreased vimentin in Rig-G expressing cells, supporting our hypothesis that Rig-G inhibits metastasis, at least in part, through inactivation of EMT signaling (Figure 3B).

A growing body of literature demonstrates that reorganization of filamentous actin (F-actin) occurs during EMT[14]. Through rhodamine-phalloidin staining, Rig-G expressing cells demonstrated that F-actin was clearly predominantly organized in cortical bundles, which are tightly associated with cell–cell adhesions. However, in the Rig-G non-expressing cells, F-actin assembled into thick parallel bundles, or actin stress fibers, traversing the ventral cell

surface; thus validating the role of Rig-G as an EMT regulator via actin filament remodeling (Figure 3C). Collectively, our data highlight that restoration of Rig-G in lung cancer cells is capable of inhibiting EMT.

3.4 Rig-G exerts its tumor suppressive function through p53 signaling pathway

To further interrogate the mechanism(s) mediated by Rig-G, we conducted mRNA array analysis to identify its potential targets. By comparing gene expression profiles in Rig-G expressing A549 and controls cells, we identified several candidate cancer-associated pathways, including mesenchymal-to-epithelial transition and p53 pathways. Furthermore, Gene set enrichment analysis (GSEA) revealed enrichment of cell cycle and DNA replication pathways in Rig-G overexpressing cells, strongly implicating that p53 pathway is affected by Rig-G (Figure 4A).

To further confirm our hypothesis, we measured mRNA or protein levels of p53 in A549 cells with or without Rig-G overexpression. Overexpression of Rig-G substantially induced p53 expression in lung cancer cells (Figure 4B). By lung adenocarcinoma tumor microarray analysis (TMA), we found Rig-G possess a strong positive correlation with p53 expression in lung cancer tissues ($P<0.01$, Figure 4C), implying its positive impact on the p53 pathway. Subsequently, we evaluated expression alterations in several p53 targets such as p-akt, cyclin D1, p21, p-MDM2 and BCL-2. As shown in Figure 4D, the overexpression of Rig-G in A549 cells remarkably inhibited the expression of p53 downstream genes; highlighting the notion that p53 is a novel downstream target of Rig-G in lung cancer.

3.5 The suppressive effects of Rig-G is abrogated by p53 pathway inhibitor in lung cancer cells

Since p53 signaling pathway is regulated by Rig-G, it remains unclear whether inhibition of p53 can also block the biological effect of Rig-G in lung cancer cells. To this end, we treated Rig-G expressing A549 cells and corresponding control cells with or without, a p53 inhibitor Pifithrin-α (PFTα). Although Rig-G overexpression alone strikingly inhibited cell growth and migration, the addition of PFTα caused significant alleviation of this biological suppression by Rig-G, highlighting that its activity requires p53 involvement (Figure 5A–B).

Finally, to study the impact of PFTα on Rig-G-mediated p53 activation, we treated A549 cells with either Rig-G overexpression alone, or in combination with PFTα. Notwithstanding the fact that increased Rig-G expression up-regulated E-cadherin and p21 expression and simultaneously inhibited vimentin expression, PFTα, on the other hand, significantly mitigated the inhibitory effect of Rig-G on p53 and EMT pathways in lung cancer cells (Figure 5C). Accordingly, our results for the first time demonstrate that Rig-G exerts a tumor suppressive function in a p53-dependant manner in lung cancer (Figure 5D).

4. Discussion

In this study, we for the first time showed that Rig-G is downregulated in lung cancer and restoration of its expression resulted in inhibition of cell growth and metastasis, both in the cell lines, as well as an animal model Second, we unraveled a novel mechanism that Rig-G exerts its antitumor activity in a p53-depedant manner. Third, from a biological perspective,

we demonstrated that Rig-G is involved in inhibition of EMT pathway and aggressiveness of lung cancer cells, highlighting a potential therapeutic importance of Rig-G in lung adenocarcinoma.

Recently, Rig-G protein has gained considerable interest in view of the evidence indicating that induction of Rig-G by IFN-α occurs not only in acute promyelocytic leukemia, but also in other types of solid tumors[7, 15]. By performing a systematic and compressive multi-cohort analysis, we systematically demonstrate that loss of Rig-G expression is a frequent event in lung cancer, and its lower expression correlated with poor clinical outcome. In support of these observations, restoration of Rig-G not only successfully led to inhibition of cell growth, but as well suppression of metastasis; yet again emphasizing its tumor suppressive role in the development of lung cancer. In addition, we observed that Rig-G is able to inactivate EMT signaling to impede metastases.

To further investigate the molecular event(s) mediated by Rig-G, we performed RNA sequencing for a comprehensive pathway analysis. Intriguingly, we found that EMT and p53 pathways were the most prominent and distinctly altered cancer-related pathways in Rig-G expressing cells. Moreover, not only p53 gene per se, but other p53 downstream targets could were remarkably induced by Rig-G. Although lung cancers display a high percentage of p53 mutations (~50%) in hotspots regions, a substantial subpopulation of patients with wild type p53 have a relatively low expression of this tumor suppressor[16–18]. Therefore, much still remains to be explore for deciphering specific mechanism(s) for p53 inactivation. In the present study, we found that overexpression of Rig-G can reactivate p53 expression in p53 wild type A549 and NCI-H1944 cells, indicating that Rig-G is one of important p53 inducers in lung cancer. Recent studies have elegantly demonstrated that p53 activity is primarily controlled by the ubiquitin E3 ligase, such as MDM2, RING1, COP1, etc., which targets p53 for proteasomal degradation[19–21]. Coincidentally, it was reported that Rig-G could regulate activity of SCF (Skp1-Cul1-F-box protein)-E3 ligase and inhibit ubiquitin-mediated protein degradation[22], which yet again supports the notion that Rig-G probably mediates p53 degradation by targeting a E3 ligase. Although further data are needed to confirm this hypothesis; our study revealed a novel mechanism that Rig-G participates in the activation of p53 signaling pathway in lung cancer.

To better appreciate the biological role of Rig-G-p53 axis for its contribution towards lung carcinogenesis, we used a p53 inhibitor, PTFα, to determine whether the suppressive effects of Rig-G are p53 dependent. Indeed, Rig-G failed to inhibit cell growth, migration or EMT when lung cancer cells were simultaneously treated with PTFα. Several studies have revealed interaction of p53 with EMT core transcription factors, such as snail and slug, which control onset and progression of the EMT cascade[23, 24]. Furthermore, activated p53 is sufficient to initiate the reversal of mesenchymal cells to an epithelial phenotype, thereby inhibiting tumor metastasis[25] and supporting our results that blocking p53 signaling abrogates inhibitory effects of Rig-G on EMT. Finally, since p53 provides a central hub linking multiple biological process, its inhibition inevitably affects the function of Rig-G in lung cancer cells.

Non-small cell lung cancer is the most common type of lung cancer (~ 80% of lung cancers). The main subtypes of NSCLC include adenocarcinoma, squamous cell carcinoma and Large cell carcinoma. The limitation of our study is we investigated Rig-G's role only in adenocarcinoma. Since inhibition of p53 or activating EMT are common molecular events for promoting lung cancer development, we hypothesized that Rig-G may exert its suppressive effect through p53 and EMT in other subtypes of NSCLC as well. However, this hypothesis needs to be confirmed in cancer tissues or cell lines derived from other subtypes of lung cancer.

5. Conclusion

Ours is the first study to systematically and comprehensively interrogate the functional and clinical significance of Rig-G and its novel target p53 in lung cancer. We concluded that restoration of Rig-G is a promising therapeutic strategy to restore p53 tumor suppressive function in lung cancer, which may potentially benefit patients with metastatic disease.

Funding:

The present work was supported by the grants R01 CA72851, CA181572, CA184792, CA202797, and U01 CA187956 from the National Cancer Institute, National Institutes of Health, pilot grants from the Baylor Sammons Cancer Center and Foundation, funds from the Baylor Scott & White Research Institute and financial support from the Beckman Research Institute of City of Hope, to Ajay Goel. This work was also supported by grants 81272603, 81472179 and 81873975 from National Natural Science Foundation of China, grant 2018BR31 from Excellent Academic Leader Training Program of Shanghai Health System, and grant ITJ(ZD) 1803 from Clinical Research and Cultivation Project of Shanghai Tongji Hospital to Dong Li. In addition, this work was supported by grants 81672826 and 81874179 from the National Natural Science Foundation of China, grant 2017YQ044 from Municipal Human Resources Development Program for Outstanding Young Talents in Medical and Health Sciences in Shanghai, and grant 18PJD047 from Shanghai Pujiang Talent Plan to Wenhao Weng.

Abbreviations

Rig-G	Retinoic Acid-Induced G
EMT	epithelial-mesenchymal transition
ATRA	all-trans retinoic acid
IFNα	interferon α
ATCC	the American Type Tissue Collection
DMEM	Dulbecco's modified Eagle's medium
FBS	fetal bovine serum
SI	staining intensity
PP	percentage of positive cells
TMA	tumor microarray analysis
GSEA	Gene set enrichment analysis
RNA-seq	RNA sequencing

PFTα	Pifithrin-α

References

1. Bray F, Ferlay J, Soerjomataram I, Siegel RL, Torre LA, Jemal A. Global cancer statistics 2018: GLOBOCAN estimates of incidence and mortality worldwide for 36 cancers in 185 countries. CA Cancer J Clin 2018;68: 394–424. [PubMed: 30207593]
2. Cao M, Chen W. Epidemiology of lung cancer in China. Thorac Cancer 2018.
3. Agustoni F, Suda K, Yu H, Ren S, Rivard CJ, Ellison K, Caldwell C Jr., Rozeboom L, Brovsky K, Hirsch FR EGFR-directed monoclonal antibodies in combination with chemotherapy for treatment of non-small-cell lung cancer: an updated review of clinical trials and new perspectives in biomarkers analysis. Cancer Treat Rev 2018;72: 15–27. [PubMed: 30445271]
4. Wu SG, Shih JY. Management of acquired resistance to EGFR TKI-targeted therapy in advanced non-small cell lung cancer. Mol Cancer 2018;17: 38. [PubMed: 29455650]
5. Giroux DJ, Rami-Porta R, Chansky K, Crowley JJ, Groome PA, Postmus PE, Rusch V, Sculier JP, Shepherd FA, Sobin L, Goldstraw P, International Association for the Study of Lung Cancer International Staging C. The IASLC Lung Cancer Staging Project: data elements for the prospective project. J Thorac Oncol 2009;4: 679–83. [PubMed: 19461401]
6. Yu M, Tong JH, Mao M, Kan LX, Liu MM, Sun YW, Fu G, Jing YK, Yu L, Lepaslier D, Lanotte M, Wang ZY, et al. Cloning of a gene (RIG-G) associated with retinoic acid-induced differentiation of acute promyelocytic leukemia cells and representing a new member of a family of interferon-stimulated genes. Proc Natl Acad Sci U S A 1997;94: 7406–11. [PubMed: 9207104]
7. Kim HJ, Lotan R. Identification of retinoid-modulated proteins in squamous carcinoma cells using high-throughput immunoblotting. Cancer Res 2004;64: 2439–48. [PubMed: 15059897]
8. Lou YJ, Pan XR, Jia PM, Li D, Xiao S, Zhang ZL, Chen SJ, Chen Z, Tong JH. IRF-9/STAT2 [corrected] functional interaction drives retinoic acid-induced gene G expression independently of STAT1. Cancer Res 2009;69: 3673–80. [PubMed: 19351818]
9. Li D, Sun J, Liu W, Wang X, Bals R, Wu J, Quan W, Yao Y, Zhang Y, Zhou H, Wu K. Rig-G is a growth inhibitory factor of lung cancer cells that suppresses STAT3 and NF-kappaB. Oncotarget 2016;7: 66032–50. [PubMed: 27602766]
10. Xiao S, Li D, Zhu HQ, Song MG, Pan XR, Jia PM, Peng LL, Dou AX, Chen GQ, Chen SJ, Chen Z, Tong JH. RIG-G as a key mediator of the antiproliferative activity of interferon-related pathways through enhancing p21 and p27 proteins. Proc Natl Acad Sci U S A 2006;103: 16448–53. [PubMed: 17050680]
11. Bhattacharjee A, Richards WG, Staunton J, Li C, Monti S, Vasa P, Ladd C, Beheshti J, Bueno R, Gillette M, Loda M, Weber G, et al. Classification of human lung carcinomas by mRNA expression profiling reveals distinct adenocarcinoma subclasses. Proc Natl Acad Sci U S A 2001;98: 13790–5. [PubMed: 11707567]
12. Kellar A, Egan C, Morris D. Preclinical Murine Models for Lung Cancer: Clinical Trial Applications. Biomed Res Int 2015;2015: 621324. [PubMed: 26064932]
13. Smith BN, Bhowmick NA. Role of EMT in Metastasis and Therapy Resistance. J Clin Med 2016;5.
14. Haynes J, Srivastava J, Madson N, Wittmann T, Barber DL. Dynamic actin remodeling during epithelial-mesenchymal transition depends on increased moesin expression. Mol Biol Cell 2011;22: 4750–64. [PubMed: 22031288]
15. de Veer MJ, Sim H, Whisstock JC, Devenish RJ, Ralph SJ. IFI60/ISG60/IFIT4, a new member of the human IFI54/IFIT2 family of interferon-stimulated genes. Genomics 1998;54: 267–77. [PubMed: 9828129]
16. Gibbons DL, Byers LA, Kurie JM. Smoking, p53 mutation, and lung cancer. Mol Cancer Res 2014;12: 3–13. [PubMed: 24442106]
17. Kim DW, Kim KC, Kim KB, Dunn CT, Park KS. Transcriptional deregulation underlying the pathogenesis of small cell lung cancer. Transl Lung Cancer Res 2018;7: 4–20. [PubMed: 29535909]

18. Merkel O, Taylor N, Prutsch N, Staber PB, Moriggl R, Turner SD, Kenner L. When the guardian sleeps: Reactivation of the p53 pathway in cancer. Mutat Res 2017;773: 1–13. [PubMed: 28927521]

19. Ka WH, Cho SK, Chun BN, Byun SY, Ahn JC. The ubiquitin ligase COP1 regulates cell cycle and apoptosis by affecting p53 function in human breast cancer cell lines. Breast Cancer 2018;25: 529–38. [PubMed: 29516369]

20. Zhao K, Yang Y, Zhang G, Wang C, Wang D, Wu M, Mei Y. Regulation of the Mdm2-p53 pathway by the ubiquitin E3 ligase MARCH7. EMBO Rep 2018;19: 305–19. [PubMed: 29295817]

21. Shen J, Li P, Shao X, Yang Y, Liu X, Feng M, Yu Q, Hu R, Wang Z. The E3 Ligase RING1 Targets p53 for Degradation and Promotes Cancer Cell Proliferation and Survival. Cancer Res 2018;78: 359–71. [PubMed: 29187402]

22. Xu GP, Zhang ZL, Xiao S, Zhuang LK, Xia D, Zou QP, Jia PM, Tong JH. Rig-G negatively regulates SCF-E3 ligase activities by disrupting the assembly of COP9 signalosome complex. Biochem Biophys Res Commun 2013;432: 425–30. [PubMed: 23415865]

23. Lee SH, Lee SJ, Jung YS, Xu Y, Kang HS, Ha NC, Park BJ. Blocking of p53-Snail binding, promoted by oncogenic K-Ras, recovers p53 expression and function. Neoplasia 2009;11: 22–31, 6p following [PubMed: 19107228]

24. Shiota M, Izumi H, Onitsuka T, Miyamoto N, Kashiwagi E, Kidani A, Hirano G, Takahashi M, Naito S, Kohno K. Twist and p53 reciprocally regulate target genes via direct interaction. Oncogene 2008;27: 5543–53. [PubMed: 18504427]

25. Powell E, Piwnica-Worms D, Piwnica-Worms H. Contribution of p53 to metastasis. Cancer Discov 2014;4: 405–14. [PubMed: 24658082]

Novelty and Impact:

The role of Rig-G in lung cancer remains unknown. Herein, the author first showed Rig-G is down-regulated in lung cancer tissues and its low expression is correlated with key clinico-pathological features and survival outcomes in a multi-site clinical cohort of 300 lung cancer patients. Biologically, Rig-G functions as tumor suppressor in lung cancer cells by *in vivo* and *in vitro* studies. Furthermore, p53 pathway is identified as a new downstream target of Rig-G.

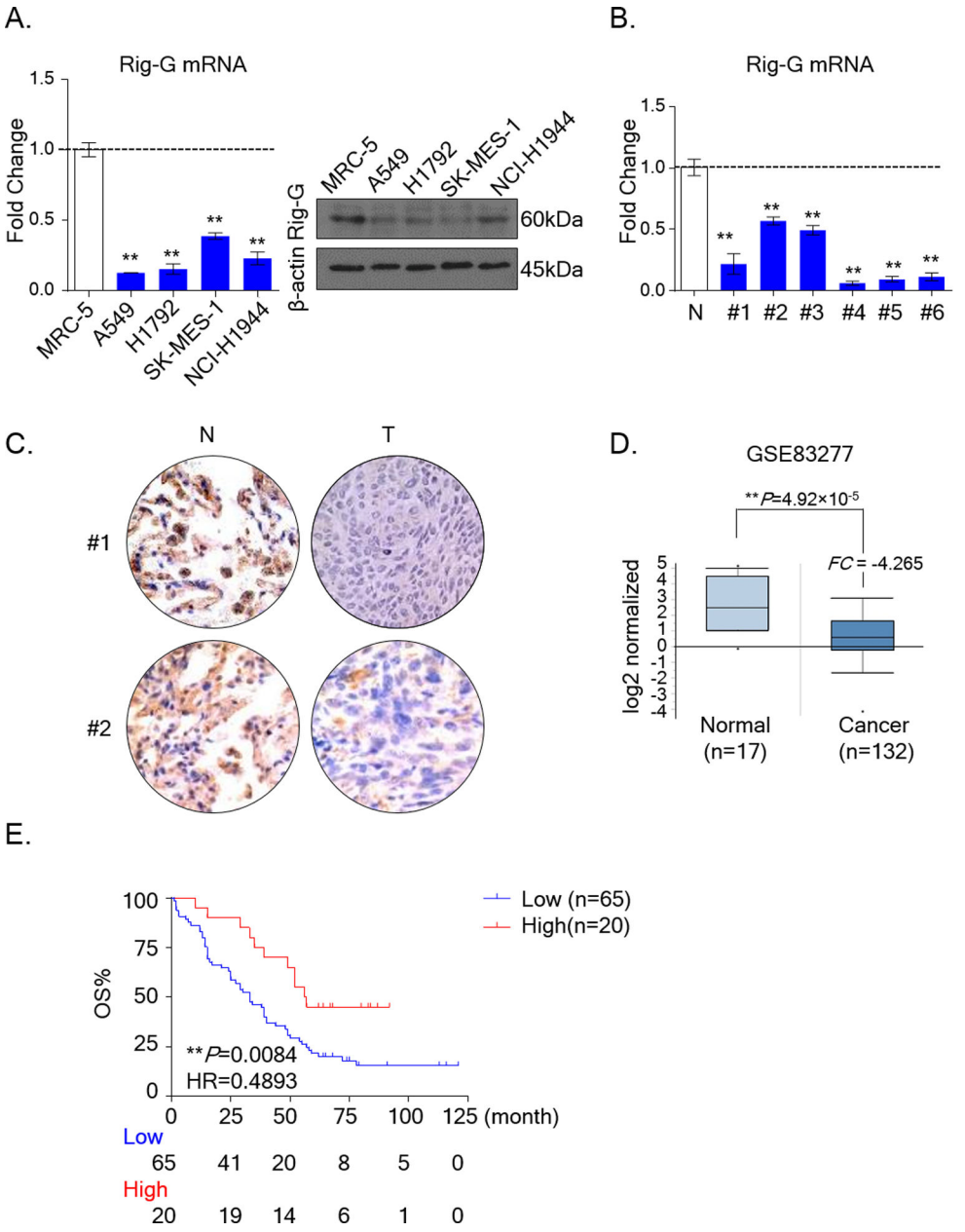

Figure 1: The clinical significance of Rig-G in lung cancers and cell lines

A) The mRNA (Left) and protein (Right) expression levels of Rig-G are lower in lung cancer cell lines (A549, H1792, SK-MES-1 and NCI-H1944), compared to normal lung fibroblast cell line MRC-5 (**P< 0.01, Mann–Whitney U test was used to compare lung cancer cells and control MRC-5 cells). **B)** The relative fold expression levels of Rig-G were accessed in lung cancer and matched healthy tissues by qPCR (**P< 0.01, Mann–Whitney U test was used to compare cancer tissues and healthy tissues). **C)** Representative IHC images for Rig-G in lung cancer and matched healthy tissues (Patient #1 and Patient #2). **D)** The expression of Rig-G between cancer and normal was evaluated in an independent microarray dataset (GSE83277) using Oncomine. **E)** The OS (overall survival) analysis was performed by Kaplan–Meier test and the log-rank method. HR: Hazard Ratio.

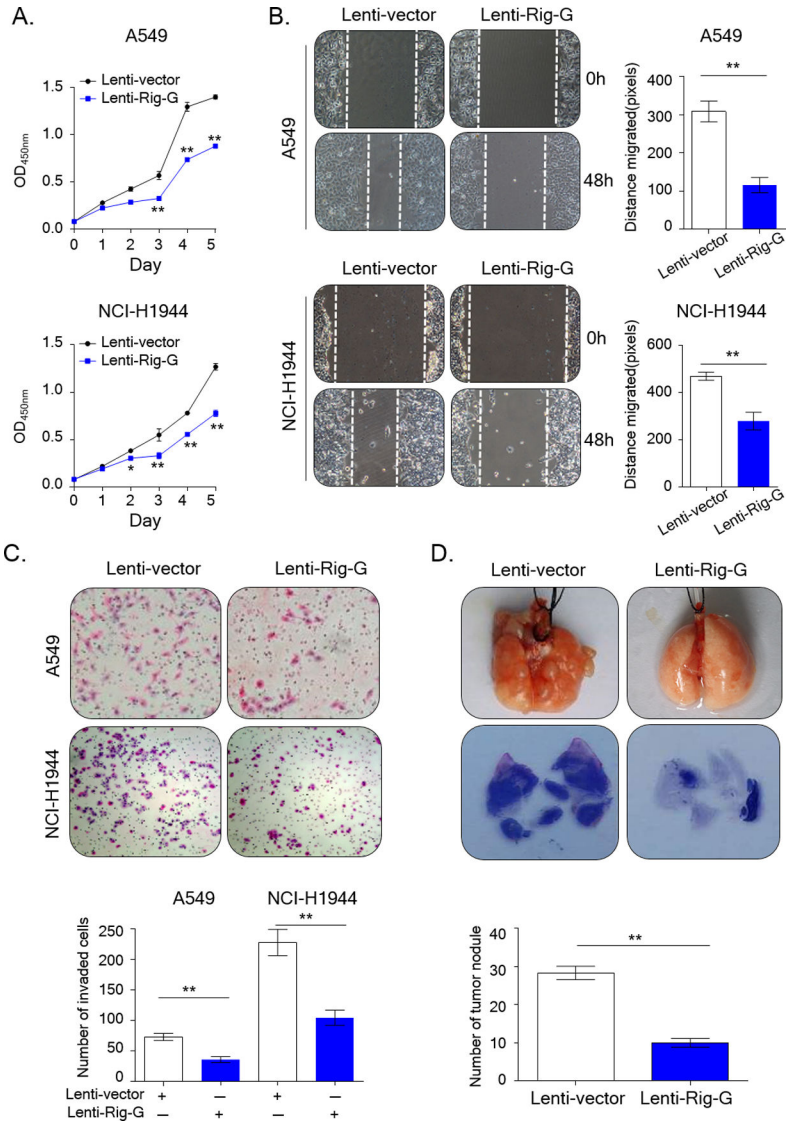

Figure 2: Overexpression of Rig-G results in the suppression of cell growth and migration in lung cancer cells cultured cells and an animal model

A) CCK-8 assay was performed in A549 (up) and NCI-H1944 (bottom) cells with or without Rig-G overexpression (n=3, **P*< 0.05, ***P*< 0.01, unpaired Student t testwas used to compare control and treated cells). **B)** The wound healing assay was performed to evaluate the invasive capability of treated or control cells (Rig-G expressing cells *vs* control cells; n=3,***P*< 0.01,unpaired Student t test). **C)** Migration assay showed Rig-G overexpression inhibited migration ability of A549 and NCI-H1944 cells (Rig-G expressing cells *vs* control cells; n=3,***P*< 0.01,unpaired Student t test). **D)** LLC cells with or without Rig-G overexpression were injected into lateral tail veins of 4–5-week-old female C57BL/6 mice. The tumors were resected 14 days after injection of LLC cells. Rig-G expressing LLC cells developed fewer lung tumor metastases compared to controls (up). For tissue morphology evaluation, hematoxylin and eosin staining was performed in paraffi embedded tissue sections (bottom;Rig-G expressing cells *vs* control cells; n=3,***P*< 0.01,Mann–Whitney U test test).

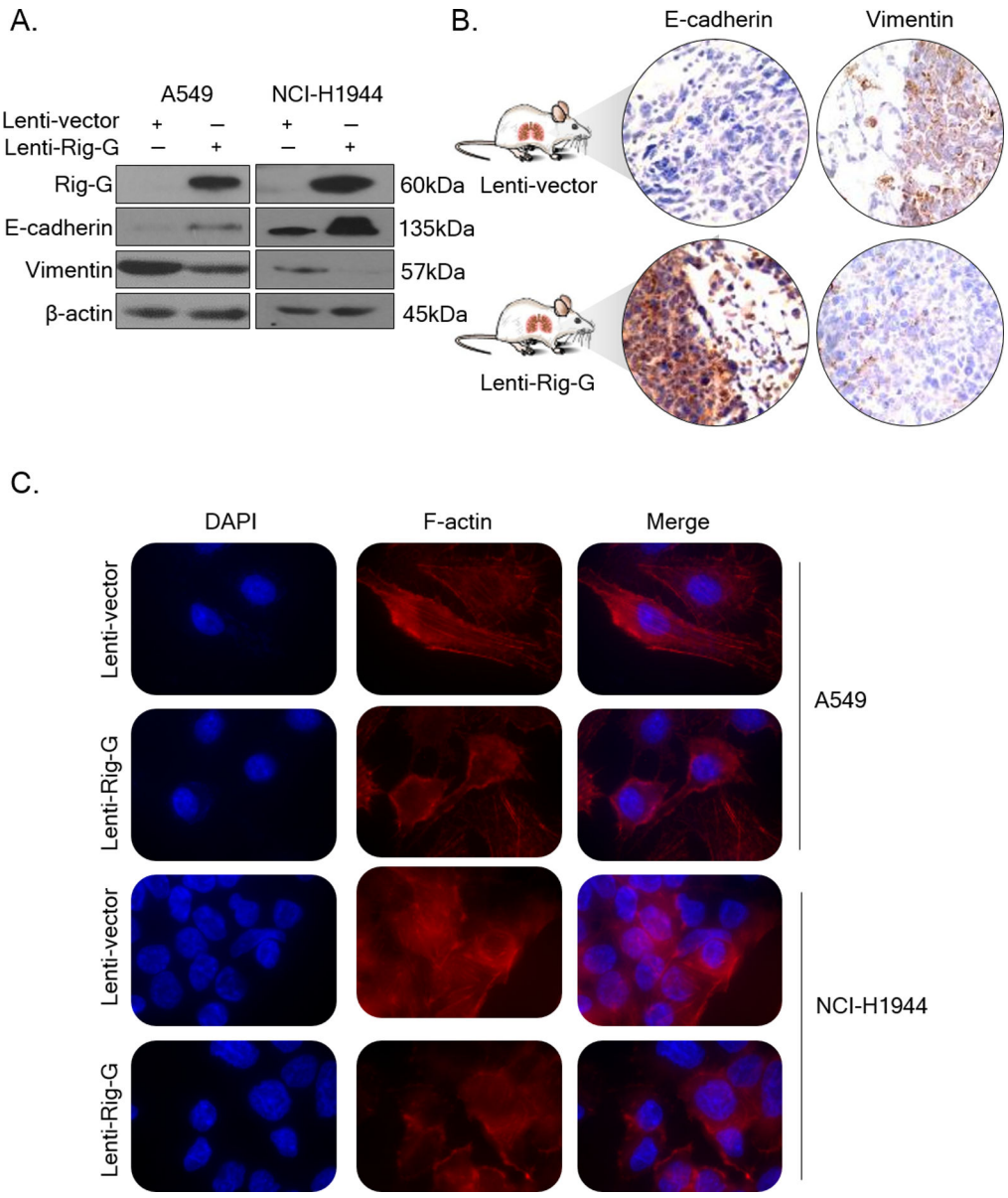

Figure 3: Overexpression of Rig-G inhibits epithelial-mesenchymal transition in lung cancer cells

A) Western blotting assay demonstrating the expression levels of epithelial-mesenchymal transition markers in A549 and NCI-H1944 cells with or without Rig-G overexpression. **B)** Representitive images of immunofluorescence staining for F-actin in control or treated cells.

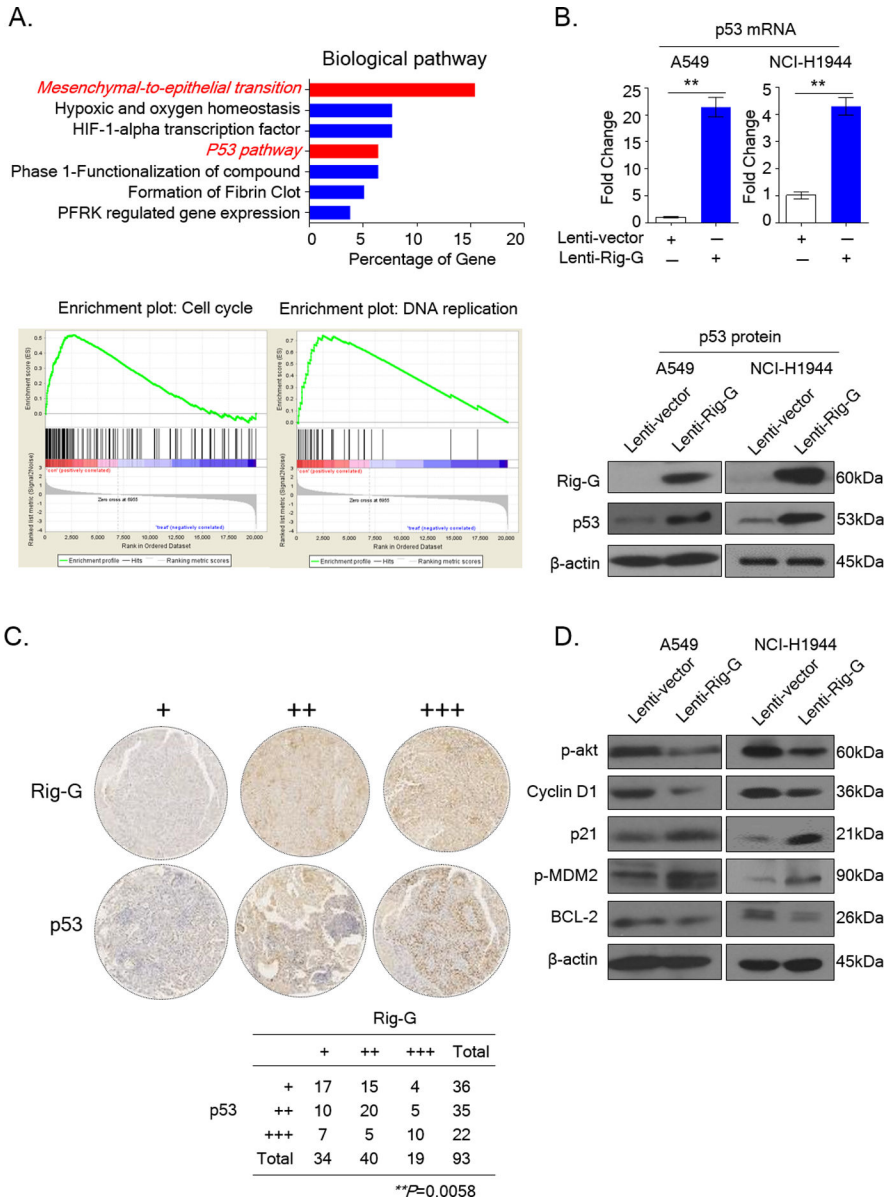

p53 \ Rig-G	+	++	+++	Total
+	17	15	4	36
++	10	20	5	35
+++	7	5	10	22
Total	34	40	19	93

Figure 4: p53 pathway is downstream target of Rig-G in lung cancer

A) p53 pathway is affected by Rig-G overexpression in A549 cells. Biological pathway analysis and gene set enrichment analysis (GSEA) was used to identify potential downstream targets of Rig-G in lung cancers. **B)** qPCR (up) and Western blotting (down) was used to access mRNA and protein levels of p53 in A549 with or without Rig-G overexpression (Rig-G expressing cells *vs* control cells; n=3,** $P< 0.01$, unpaired Student t test). **C)** The expression correlation of p53 and Rig-G in lung tissue microarray (n=93, ** $P<0.05$, chi square ($\chi 2$) test). **D)** Western blotting was used to evaluate expression of p53 downstream targets in A549 cells with or without Rig-G overexpression.

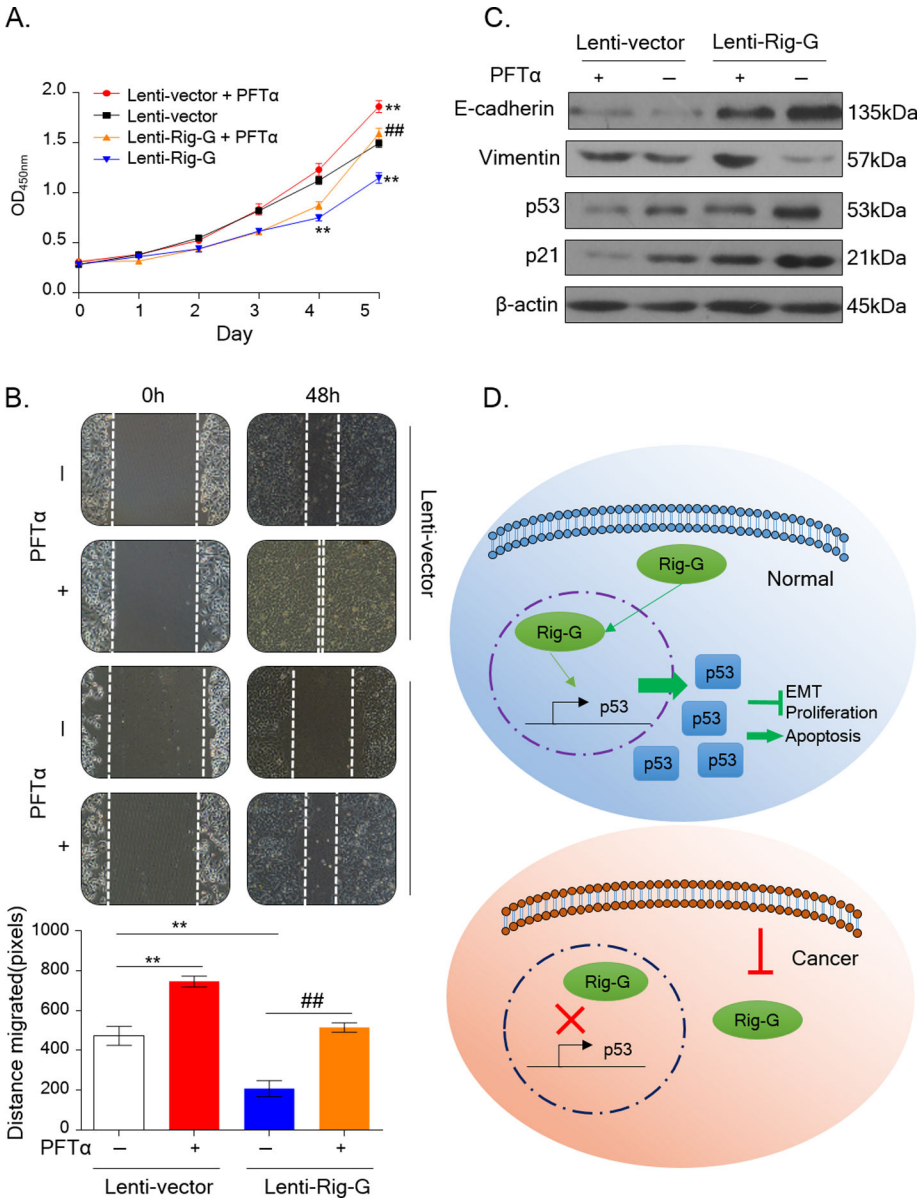

Figure 5: The suppressive effects of Rig-G is abrogated by p53 inhibitor Pifithrin-α (PFTα) in lung cancer cells PFTα inhibits tumor-suppressive effects of Rig-G in vitro. CCK-8

(A) and wound healing assays **(B)** were performed in A549 with Rig-G overexpression alone, PFTα treatment alone, or both (n=3, $^{**}P<0.01$, treated cells *vs* Rig-G non-expressing control cells; $^{\#\#}P<0.01$, both Rig-G and PFTα treated cells *vs* Rig-G overexpression alone treated cells; unpaired Student t test). **C)** Western blotting illustrating PFTα reduced inhibitory effect of Rig-G on p53 and EMT pathways in A549 cells. **D)** A proposed mechanistic model depicting how Rig-G functions as a tumor suppressor and regulates EMT via promoting p53 pathway in lung cancer.

Table 1:

The correlation of Rig-G1 expression and clinicopathological variables in patients with lung adenocarcinoma.

Variables		n	Low (n=73)	High (n=18)	*P*
Age	≤60	47	38	9	0.87688
	>60	44	35	9	
Gender	female	51	44	7	0.10155
	male	40	29	11	
Grade	I/II	60	50	10	0.29959
	III/IV	31	23	8	
Stage	I/II	61	43	18	**0.00089
	III/IV	30	30	0	
Lymph node metastasis	negative	79	62	17	0.28544
	positive	12	11	1	

** *P*<0.01